CHAPTER 1
INTRODUCTION

1.1 BACKGROUND OF STUDY

Natural has (NG) has been gaining attention to be used as fuel for combustion engines. Methane is the major constituent in natural gas. It represents about 95%. Natural gas is more environment friendly compared to other conventional fuel [1-7].

Adsorbed Natural Gas (ANG) is an attractive alternative to replace Compressed Natural Gas (CNG) storage in the near future as in the vehicle application. The traditional way of natural gas storage, CNG suffers from various problems. For instance, the need of high pressure (up to 25 MPa) for the use in natural gas fuelled vehicle [1]. The large cost of cylinders used for storage and the high pressure facilities necessary limit the wide spread of CNG [1].

Therefore, the technology of ANG is an alternative in which adsorb natural gas up to 3.4MPa takes place [1]. However, because its equivalent storage in comparison with CNG is quite low, consequently the adsorbent must possess the feature of high methane uptake per volume [1]. Among all types of adsorbent, activated carbon is proven to have a high potential as natural gas adsorbent due to its high porous surface area. Yet, the ideal activated carbon has the features of high adsorption capacity, good mechanical cohesion, good heat transfer properties, good mass transfer properties and uniform pore distribution. [3] Hence, many researches have been done to characterize and study the suitable adsorbents for high methane adsorption capacity.

1.2 PROBLEM STATEMENT

There are various kinds of adsorbent material for natural gas storage. One of them is activated carbon. The behaviour of these materials during gas charging differs according to the nature of that material and operating conditions. Other than that, due to the different features vary along with different types of adsorbent, such as the material surface characteristics, this would also give a variation on the adsorption quantity. This project is to study the charging cycle of methane on activated carbon at different charge pressure, flow rate and adsorbent surface characteristics.

1.3 SIGNIFICANCE OF THE PROJECT

This project is very useful and serves as a reference on ANG research in the future. For instance, some related companies may use this research as a reference for their selection and design of natural gas adsorbent for vehicle storage. Even some companies or students in the university can further the research to solve in the related researches.

1.4 OBJECTIVES AND SCOPE OF STUDY

There are two objectives in this project. The first one is to characterize the adsorbent material. Two types of activated carbon are used in this project. The second objective is to study the behaviour profiles which are thermal profile, period of charging and adsorption capacity during the charging phase at different charge pressure and flow rate of methane.

The scope of study will cover various charging experiments in a vertical cylinder to obtain the methane adsorption capacity, the period of charging and thermal behaviour during charging. Two activated carbons are used and characterized to determine the surface morphology, pore size, micropore volume, micropore area and specific surface area.

1.5 RELEVANCY OF THE PROJECT

This project is relevant to the recent concern of using ANG for light duty vehicle. The ANG researchers are still finding the most suitable adsorbent for optimum storage at reasonable temperature and pressure. This research is to study the charging behaviour of the adsorbents for actual application in natural gas storage for light duty vehicle.

1.6 FEASIBILITY OF THE PORJECT

The project is feasible provided that UTP could provide the materials and equipments requested on time. The cost of the project is estimated to be low. The activated carbons used are commercial activated carbon and can be obtained at low price. This project will bring a big benefit in the industry and made as a future reference in ANG research.

CHAPTER 2
LITERATURE REVIEW

2.1 THE IDEAL PROPERTIES OF ADSORBENT

The properties of ideal activated carbon are:

- High adsorption capacity which depends on the packing density and microporous volume [4].
- Good mechanical cohesion which means able to withstand erosion and abrasion [4].
- Good heat transfer and mass transfer properties [4].
- Adsorbent with pore size at least 0.76nm to maximize the delivery at ambient pressure [11].
- Adsorbent with high surface area but low mesoporosity. The presence of low mesoporosity (< 5nm) serves as an easy access for the adsorbate molecules to travel to micropores. This form of mesopore is feeder pore [11].
- The adsorbent possesses low adsorption heat, high heat capacity [11].
- The adsorbent is hydrophobic [11].

Micropore volume and pore size distribution could be the determining factor with the condition that the solid surface is perfectly hydrophobic [5]. Surface chemistry and methane adsorption equilibria must be considered in the decision for choosing an adsorbent for natural gas storage [5]. In order to determine the hydrophobic and hydrophilic nature of the adsorbent, X-Ray Photoelectronic Spectroscopy (XPS) can be used to reveal this property [5].

2.2 ADSORBENT CHARACTERIZATION

Adsorbents are usually porous. The pore widths of porous adsorbents are classified by the International Union of Pure and Applied Chemistry (IUPAC) as micropores with pore diameters between 0.3 and 2 nm, mesopores with pore diameters between 2 and 50 nm, and macropores with pore diameter greater than 50 nm [9]. The parameters which characterize a porous adsorbent are: specific surface area, denoted by *S*, measured in m^2/g; the micropore volume, denoted by W^{MP}, measured in cm^3/g; the pore volume, denoted by W, which is the sum of the micropore and mesopore volumes of the adsorbent, measured in cm^3/g; and the pore size distribution (PSD) [9]. The PSD is graphical representation of $\Delta V_p/\Delta D_p$ versus ΔD_p, where V_p is the pore volume accumulated up to the pore of width D_p, measured in cc-STP/g.Å [9].

Gas adsorption measurements are used to characterize the porous surface and the porosity [1-7]. This method is applied for determination of the surface area, pore volume, and pore size distribution (PSD) of porous materials [1-7]. The adsorption process occurs more or less as follows [10]: firstly, the micropore will be filled which the adsorbate and the pore wall are interacting; in the later stage at higher pressure, will be the external surface coverage which is described by the adsorption on the mesopores and macropores, and at the meantime capillary condensation is happening at the mesopores.

2.2.1 The t-Plot Method

Micropore volume of porous material can be determined by t-plot method. The adsorbed thickness, t is a function of the adsorbed amount [10]. Graph n_a versus t in (Angstrom) need to be plotted to calculate the microporous volume and the outer area. t is calculated using formula for a good value $x = P/P_o$ and the amount adsorbed is taken from the experimental isotherm [10]. After plotting, points that do not fit linear plot will be eliminated with by applying the following linear Equation 2.1 [10].

(2.1)

$$y = n_a = Rt + N_a = mx + b$$

Applying Gurvich rule through the relation below to calculate microporous volume [10]

$$W^{MP} = N_a V_L \tag{2.2}$$

2.2.2 The BET Method

The BET theory, a multilayer adsorption, is used to determine the specific surface area, *S*. This method was developed by Brunaeur, Emmett and Teller [10]. It uses adsorption of N_2 at 77K. BET isotherm equation can be used for real adsorption data. The linear form Equation 2.3 [10]

$$y = \frac{x}{n_a(1-x)} = \left(\frac{1}{N_m C}\right) + \left(\frac{C-1}{C N_m}\right) x = b + mx \tag{2.3}$$

Where $x = P/P_o$.

Later, the specific surface area can be calculated using Equation 2.4 [10]:

$$S = N_m N_A \sigma \tag{2.4}$$

This method is applicable for cases where the adsorbates do not adsorbed to primary porosity; instead the adsorption occurs at the outer surface. As a result, BET equation is valid for surface area analysis of nonporous and mesoporous materials containing wide pores. However, due to microporous adsorbents is a primary porosity adsorption which is volume filling, BET theory is not applicable as BET theory describes outer surface adsorption [10].

2.3 ADSORPTION CAPACITY CALCULATION

To determine the amount of methane adsorbed on the adsorbent, it is necessary to measure the dead volume, V_d, which is the free volume (void space). V_d is the difference between V of the container and the volume V_s of the solid adsorbent [12,18].

$$V_s = \frac{m_s}{\rho_s} \tag{2.5}$$

Where $m_s$is the amount of adsorbent in V and ρ_s is the real density of the adsorbent [15].

$$V_d = V - V_s \tag{2.6}$$

The storage capacity is defined by Equation 2.7 [12]

$$Adsorbed\ capacity = \frac{Adsorbed\ methane\ (g)}{Mass\ of\ adsorbent\ (g)} \tag{2.7}$$

The moles of numbers of methane adsorbed is determined using Equation 2.8 [12]

$$n_{adsorbed} = n_T - n_d \tag{2.8}$$

The amount of gas adsorbed (mass of methane per mass of activated carbon) is determined by dividing the weight of methane adsorbed ($n_{adsorbed} \times 16.034$) with the weight of adsorbent filled in the adsorption column [12]. n_T is the number of mol of gas injected into the column, n_d is the number of mol of gas in the dead volume. n_d is determined using Equation 2.9 [12].

(2.9)

$$n_d = \frac{PV_d}{zRT}$$

Previous researches have obtained different methane adsorption capacity using different type of carbon. Table 1 shows the variation in the methane adsorption capacity at 500 psig and 298K with surface area respectively.

Table 1: Methane Adsorption Capacity of Carbon at Ambient Temperature and 34.47 barg and 298 K[11]

Carbon	**Surface Area (m^2/g)**	**Methane Capacity (mg/g)**
Carbon Lorraine	640	75
Saran (B)	900	87
Calgon SGL	900	65
PX-21, Amoco (Maxsorb)	2671	177
Electrosynthesis EL	2796	170
Maxsorb (Grade 30-SPP and Lot 92-05)	3100	211

2.4 ADSORPTION ISOTHERM

Adsorption isotherm is to show the equilibrium relationship between the concentration of adsorbate and its concentration on the adsorbent at a given temperature.

For isotherm with convex upward, it is favourable as the relative high solid loading can be achieved with low loading in the fluid. However, an isotherm with concave upward, it is not favourable which because much loading in the fluid is needed to obtain a high loading on the solid.

In normal process, the adsorption system will decrease in the amount adsorbed if the adsorption temperature is increased. Due to this reason, adsorption process is usually done at room temperature and desorption process is done at a higher temperature.

Figure 1 shows the adsorption and desorption isotherms of methane using activated carbon. It can be seen that the increase of pressue in the adsorption cell will increase the amounts of methane adsorbed. However, increasement is not significant in high pressure. This is due to the saturation of the adsorbent bed [12].

The factors that affect the adsorption capacity is the BET surface area, the pore diameter and the micropore volume [12]. The higher amount of these three factors, the higher of the methane adsorption capacity [12].

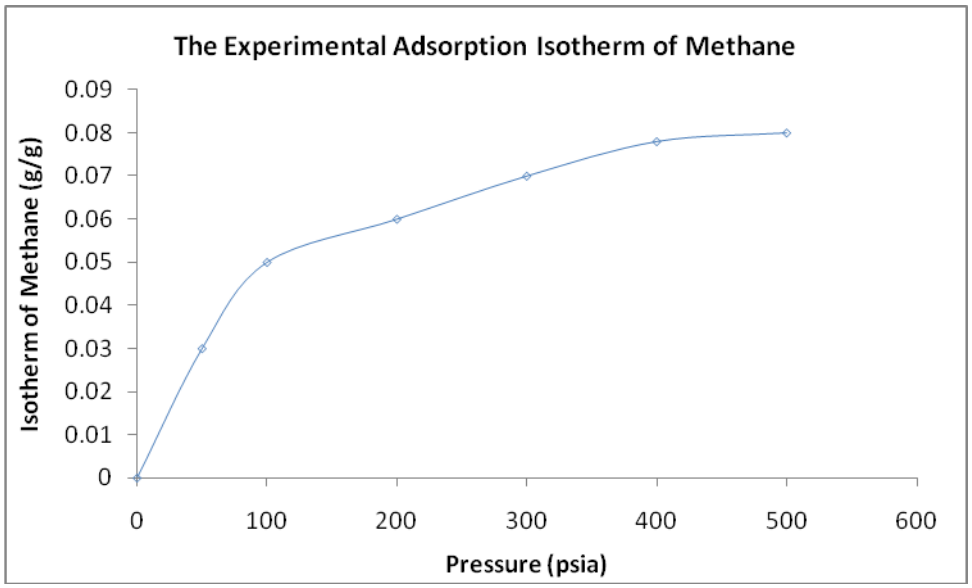

Figure 1: The Experimental Adsorption Isotherms of Methane using Activated Carbon [12]

2.5 CLASSIFICATION OF ADSORPTION ISOTHERM

Brunauer, Deming, Deming and Teller (BDDT) have introduced adsorption isotherm classification into five types in 1940. Then, IUPAC completes the adsorption isotherm classification by using BDDT as the core with another addition introduced by Sing [14]. Figure 1 is the completed set of adsorption isotherm classification [14].

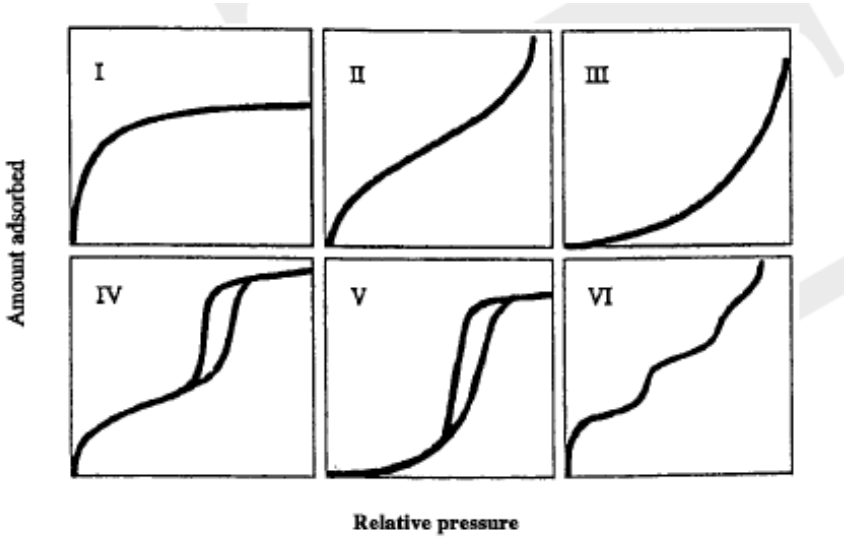

Figure 2: The IUPAC Classification for Adsorption Isotherms [14]

Type I – Adsoprtion on microporous adsorbents, monolayer coverage.

Type II – Adsorption on macroporous adsorbents with strong adsorbate-adsorbent interactions. Typical BET adsorption isotherm.

Type III - Adsorption on macroporous adsorbents with weak adsorbate-adsorbent interactions. The adsorption process is unfavorable at low pressure.

Type IV and V – Adsorption isotherms with hysteresis. Has finite limit as the pressure approaching increases due to finite pore volume of porous solids.

Type VI – Adsorption with steps.

2.6 HEAT OF ADSORPTION

During adsorption, heat is generated and it is an exothermic process. While during desorption, it requires heat and it is an endothermic process [3]. Adsorbent with high heat capacity would be good for ANG storage. Adsorbent with good thermal conductivity is desired so that heat adsorption can be easily dissipated. The heat of adsorption can be calculated using Clausis-Claypeyron equation and the adsorption isotherms at least 3 different temperatures [3].

Base of Figure 3, it is found that the temperature increased quickly to the maximum with low charging pressure [13]. Different adsorbent will behave differently during charging and discharging process [13].

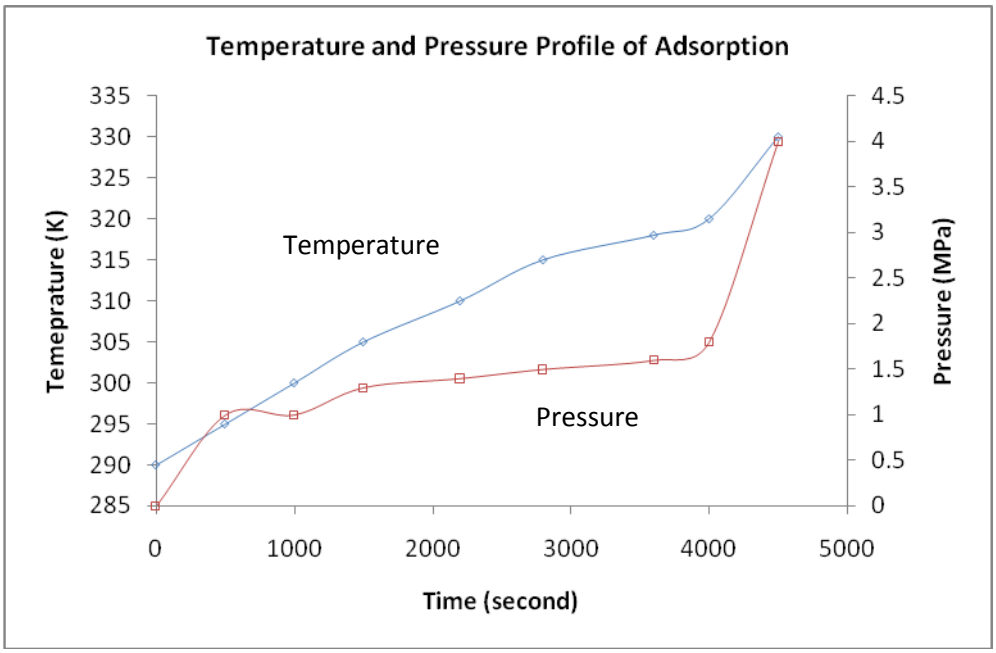

Figure 3: Adsorption Pressure and Temperature Profile [13]

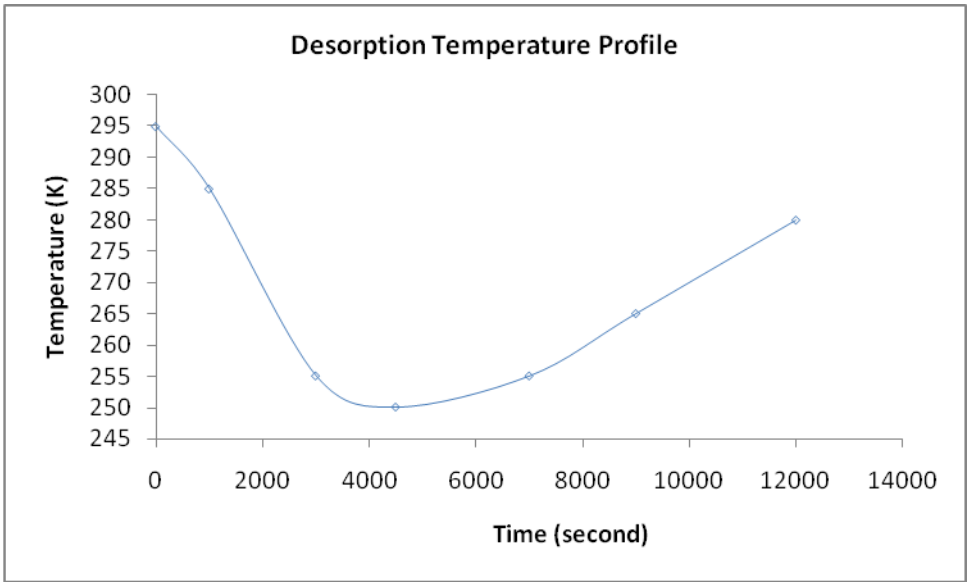

Figure 4: Desorption Temperature Profile [13]

2.7 POROUS MATERIALS

Pores are classified into two types, they are open pores and closed pores. Open pores are pores connect to the surface of the material, meanwhile closed pores are pores isolated from the outside. Materials with open pores are specially useful for adsorption. There are various shapes of pore, such as cylindrical, spherical, slit and hexagonal type. Nanoporous materials are division of porous materials, typically have pore diameters between 1 – 100 nm [9].

Nanoporous material is unique due to its high surface area, uniform pore structure, rich surface composition, large porosity and well-ordered pores [9]. Porous materials can be classified as in Table 2 [9].

Table 2: Classification of Porous Materials [9]

	Carbon	**Polymeric**	**Metal**	**Oxides**	**Alumino-silicate**
Pore Size	Micro-meso	Meso-macro	Meso-macro	Micro-meso	Micro-meso
Surface area	High 0.3-0.6	Low >0.6	Low 0.1-0.7	Medium 0.3-0.6	High 0.3-0.7
Permeability	Low-medium	Low-medium	High	Low-medium	Low
Strength	Low	Medium	Strong	Weak-medium	Weak
Thermal stability	High	Low	High	Medium-high	Medium-high
Chemical stability	High	Low	High	Very	Medium-high
Costs	High	Low	Medium	Medium	Low-medium
Life	Long	Short	Long	Long	Medium-long

The performance criteria for a good adsorbent include:

- High adsorption capacity. This parameter is determined by the specific surface area, surface chemical nature and pore size which eventually determine the amount adsorbed per unit mass adsorbent [9].
- Good mechanical properties. Adsorbents has to be strong enough to withstand the attrition, erosion and crushing during adsorption [9].
- Good stability and durability. Adsorbent often exposed to harsh chemical, pressure and thermal environment. A good stability would ensure a longer life of the adsorbent [9].

CHAPTER 3
METHODOLOGY

3.1 RESEARCH METHODOLOGY

The research methodology would start with choosing a problem statement. With the help of the problem statement, it is easy to narrow down the scope of study and find the information straight to the point. Next, is collecting data. The resources could be obtained from encyclopedia, reference books and published papers and journals. After collecting the relevant data, this data will be interpreted and analyzed. A summary or report is made for the interpretation done to take down the important information that will be helpful for the project.

3.2 EXPERIMENTAL PROJECT WORK

The project work is divided into two parts according to the objectives stated. The first part is to carry out the characterization of two types of activated carbon. The material surface morphology is observed using FESEM. The pore size, specific surface area, micropore area and micropore volume of the adsorbents are obtained using BET analyzer. The second part is the study of charging cycle of methane gas on the activated carbon using an adsorption column unit. The charging pressure is at 20, 40 and 40 bar. The charging flowrate is at 1, 2 and 3 L/min. The adsorbent materials used in the experiment are two types of commercial activated carbon.

3.2.1 Material Selection

In this project, the material selected to match the suitability of the adsorbent criteria is activated carbon. Porous carbon has pore size in the range from micropore to mesopore. Carbon material is also thermally and chemically stable. Therefore, it is strong to stand against harsh chemical and high temperature change.

Two commercial activated carbons are obtained from R&M Chemicals and Merck Company. These two activated carbons are chosen due to its avaibility in Malaysia.

3.2.2 Adsorbent Characterization

1. Field Emission Scanning Electron Microscopy (FESEM) / Scanning Electron Microsope (SEM)

   FESEM has higher resolution than Scanning Electron Microscopy (SEM). The images produced show the surface structure of the sample; the structural surface of the material, the pore size and the overview of the porosity. The imaging is done at temperature 298K. The amount of sample needed for each run is 1 g. The preparation of the sample is important to ensure it is conductive under during the imaging. As for activated carbon, no preparation on the sample has to be done as the carbon material is already conductive for imaging.

2. Surface Area Analyzer (BET)

   BET isotherm is a widely used method for extracting effective surface areas, micropore volume and pore size. Sample will be degassed overnight. The BET analyzer operates using nitrogen at 77K and atmospheric pressure. The BET equation is restricted to linearity of $\frac{1}{V}(\frac{P}{P_o-1})$ vs P/P_o, therefore the reasonable range of P/P_o from 0.01 to 0.35 [10]. The micropore volume and surface area can be determined using the t-plot method.

3.2.3 Gas Adsorption Experiment

In this study, the volumetric method was used to study the adsorption of methane on the activated carbon. The process flow diagram is shown in Figure 5. SOLTEQ Gas Adsorption Column Unit, model BP 203 is used to run the experiment. This unit comprises of an adsorption column, a gas booster pump and a vacuum pump. The gas enters adsorption column from the bottom. The column, K2 able accommodates bed height of 300mm and diameter 45mm.

For charging process, all the inlet valves to the column should be opened and all the outlet valves should be closed. In contrary, for discharging process, the gas adsorbed will be discharged to the atmospheric pressure. Therefore, all the inlet valves to the column should be closed while all the outlet valves of the column connected to the venting should be opened. To ensure the gas is fully desorbed, a vacuum pump is available to pump out the gas from the bottom of the column.

The unit is installed with pressure and temperature gauge for monitoring and process control instrumentation. The whole system is equipped with adequate safety valves (pressure relief valves) in case of overpressure. It is designed to operate within the limits of 100 bar pressure at ambient temperature. The equipment can handle temperature to 450˚C at atmospheric pressure or vacuum.

A flow controller at the inlet of the column is to adjust the flow rate to the desired value. The pressure for charging is controlled using a pressure regulator at the gas cylinder. During the experiment, the parameters to be observed are the column pressure and the column temperature.

Experiment procedure for charging the column:

1. Degassed the adsorbent (activated carbon) at 150°C for 1 hour.
2. Fill up the column, K2 with the degassed adsorbent and weigh the amount that filled the column K2.
3. Attach the column back to the system. Make sure the column is installed appropriately.
4. Purge the system with nitrogen gas, meanwhile check for leakages.
5. If no leakages, proceed with the experiment. Open the valve at the gas cylinder and regulate the pressure up to 20 bar.
6. Set the inlet flow rate to 1 L/min at FIC 04.
7. Record the initial temperature of the column, TI 05.
8. Open valve V6, V14, V15, V17, V17a and V20.
9. Start the stop watch. Record the column temperature, TI 05 and column pressure, PI 05 and PI 08 from time to time until the pressure reaches the saturation pressure (does not vary).
10. Close the inlet valves, V17 and V17a.

    Note: Maximum operating pressure is 100 bar.

Table 3: The Methane Flowrate and Pressure Setting for the Experiment

Methane Flowrate (L/min)	**Charging Pressure (bar)**
1	20
	40
	60
2	20
	40
	60
3	20
	40
	60

Start every run at temperature of 298 K.

3.3 MATERIALS AND EQUIPMENTS

Materials

- 250g Granular Activated Carbon purchased from R&M Chemicals in Malaysia.
- 250g Granular Activated Carbon from Merck Company in Malaysia.
- 1 cylinder methane gas with purity of 95%

Equipments

- FESEM/SEM for material surface imaging, available at Nano Technology Research Center, UTP.
- BET surface analyzer for material characterization available in Chemical Engineering Department.
- SOLTEQ BP 203 Gas Adsorption Column Unit for charging cycle study experiment, available in Chemical Engineering Department.

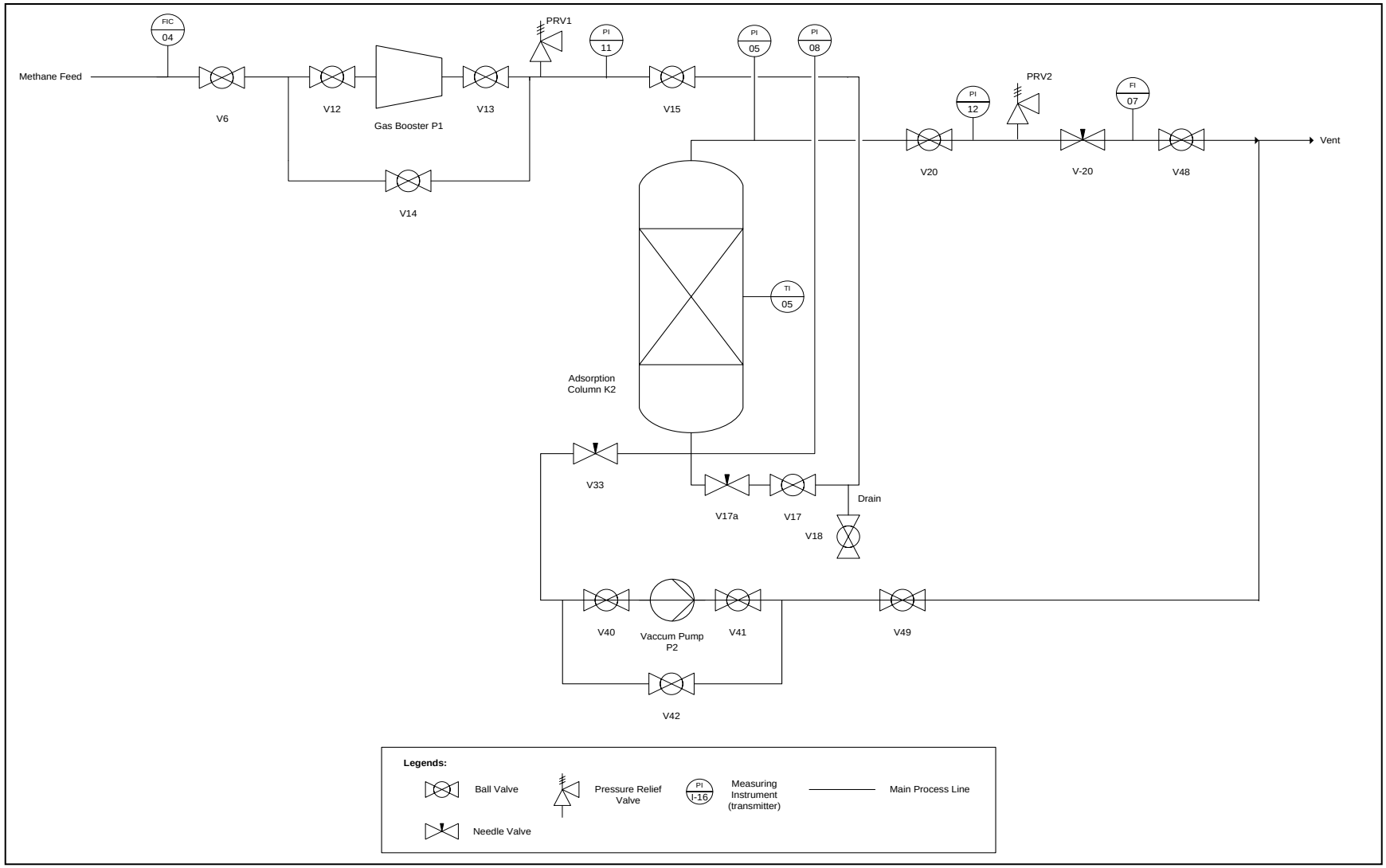

Figure 5: Process Flow Diagram for the Gas Adsorption Column Unit

CHAPTER 4
RESULT AND DISCUSSION

4.1 MATERIALS CHARACTERIZATION

4.1.1 Surface Characteristics of the Activated Carbon

Two types of granular activated carbon which are characterized using BET. The sample R&M activated carbon is named as AC1 and Merck activated carbon is named as AC2. The surface characteristics of the samples are listed in Table 4.

Table 4: Surface Characteristics of the Activated Carbon

Sample	BET Surface Area (m^2/g)	Micropore Area (m^2/g)	Micropore Volume (cm^3/g)	Average Pore Diameter (Å)
AC1	799.82	694.39	0.267	16.07
AC2	708.78	373.57	0.159	23.45

The BET surface area, t-plot micropore volume and pore size were calculated based on the nitrogen adsorption isotherms as shown in Figure 6 and 7. The volume of adsorbed gas steeply increased below $P/P_o = 0.1$ for both the activated carbon. Another steep increase also shown in AC at above $P/P_o = 0.9$. Comparing these isotherms with the BET isotherms, it was found that AC1 follows Type 1 isotherm, while AC2 follows Type 2 isotherm. The swelling at the isotherm is most probably influenced by large diameter N_2 that penetrates into the narrow pore and transform the structure. The surface area and micropore volume measurements were determined using BET plot and t-plot method respectively. Figure 8 and 9 show the BET plot for AC1 and AC2 respectively. T-plot for AC1 and AC2 are displayed in Figure 10 and 11 respectively. The values in Table 4 are calculated by the BET equipment automatically. The kinetic diameter of methane is 0.38 nm. The average pore diameter of AC1 and AC2 is twice bigger than

the size of methane, 0.76 nm. This feature would allow the gas to adsorb into the pores easily and increase the methane adsorption capacity.

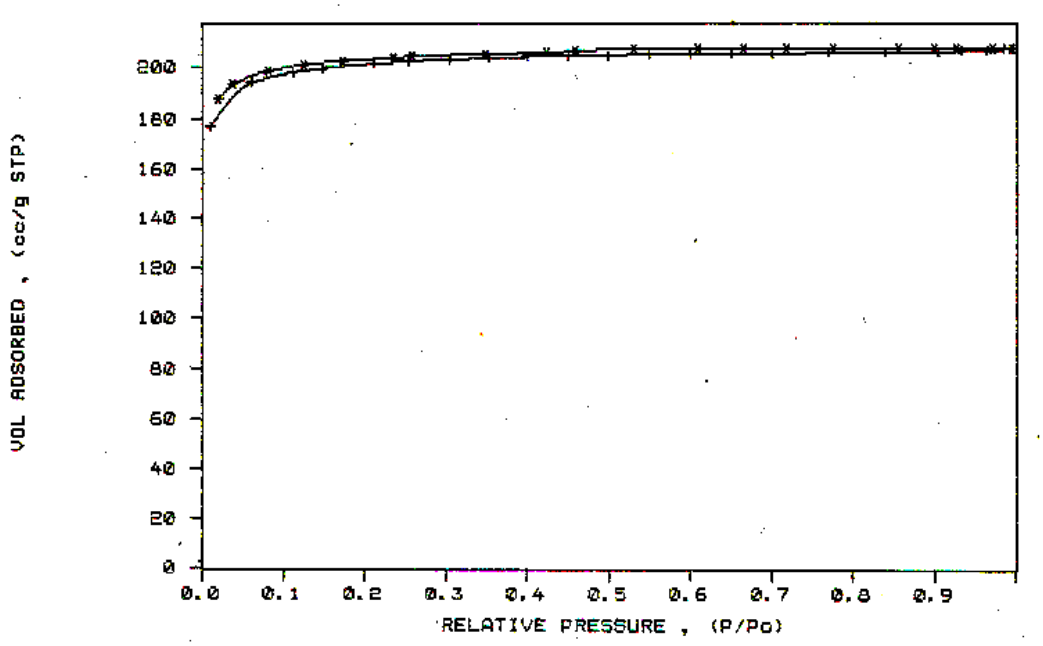

Figure 6: AC1 Nitrogen Adsorption Isotherm

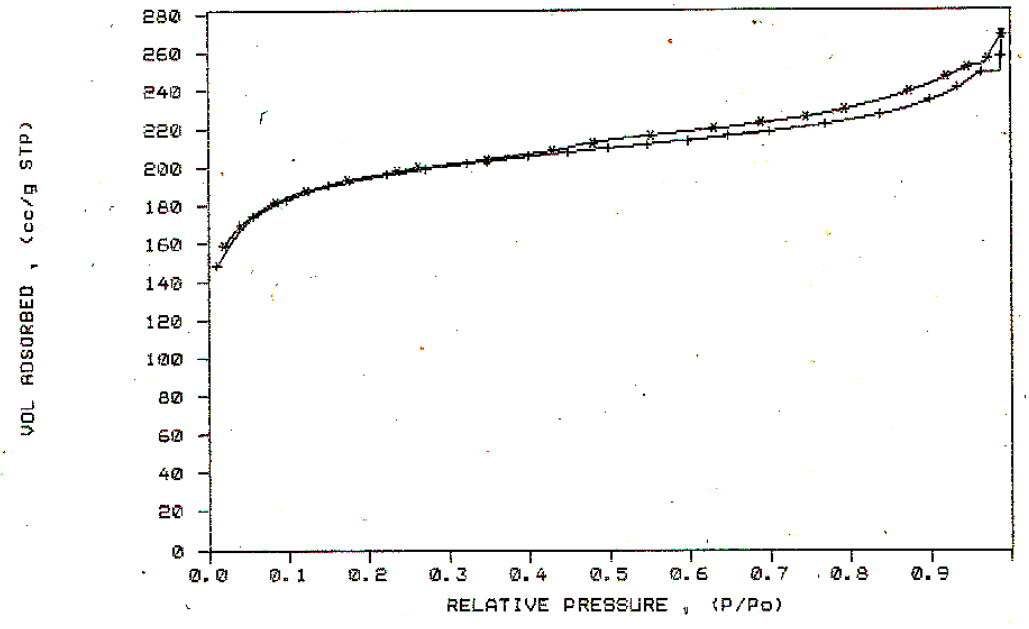

Figure 7: AC2 Nitrogen Adsorption Isotherm

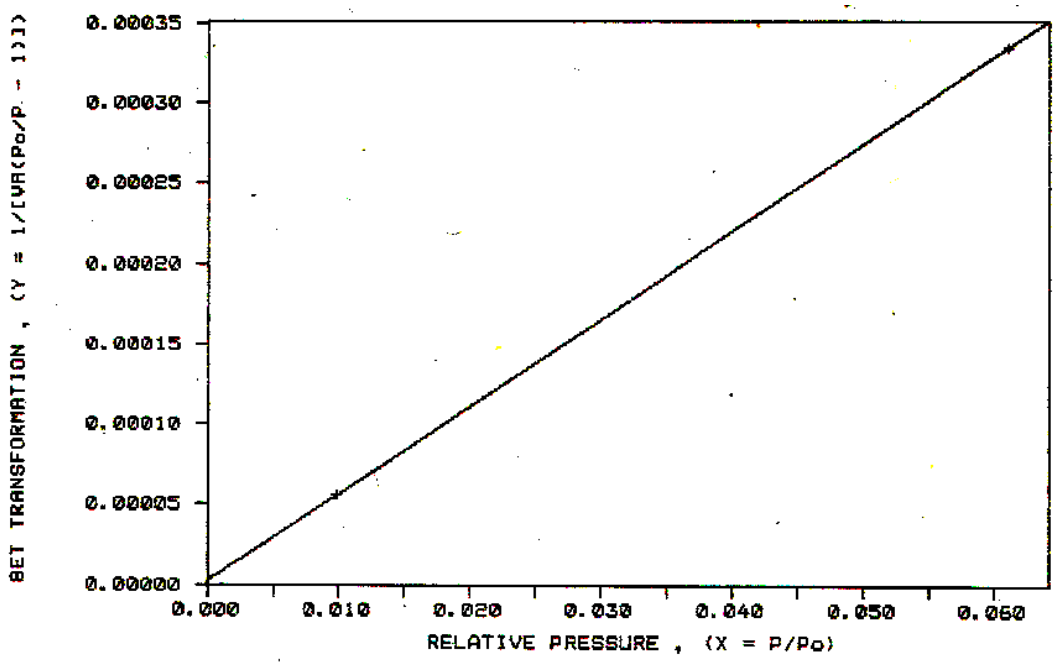

Figure 8: AC1 BET Plot

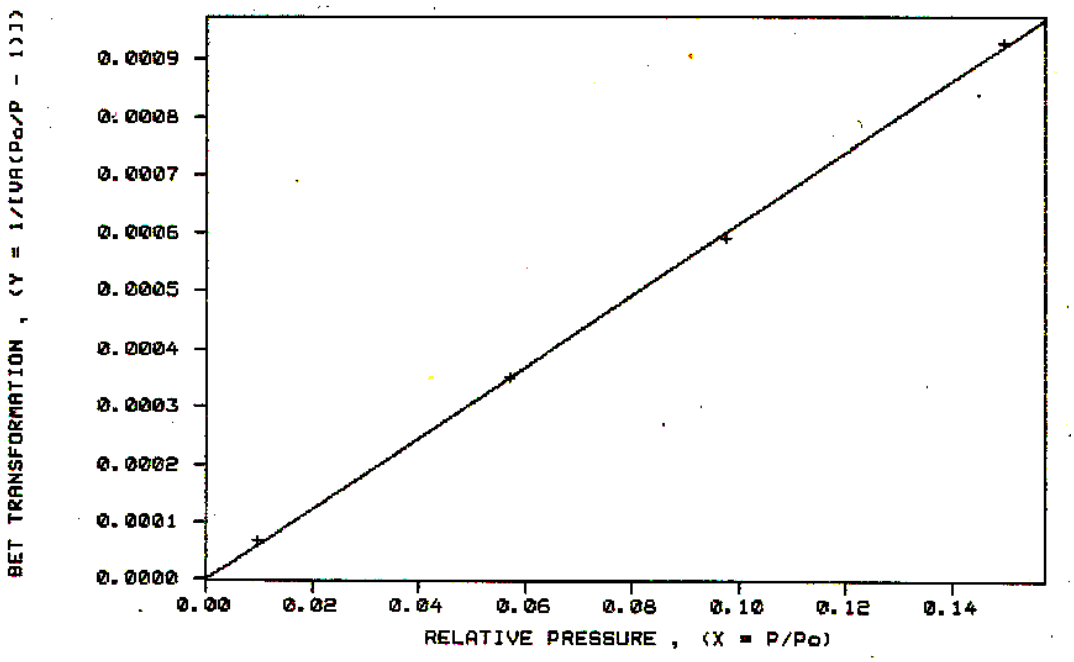

Figure 9: AC2 BET Plot

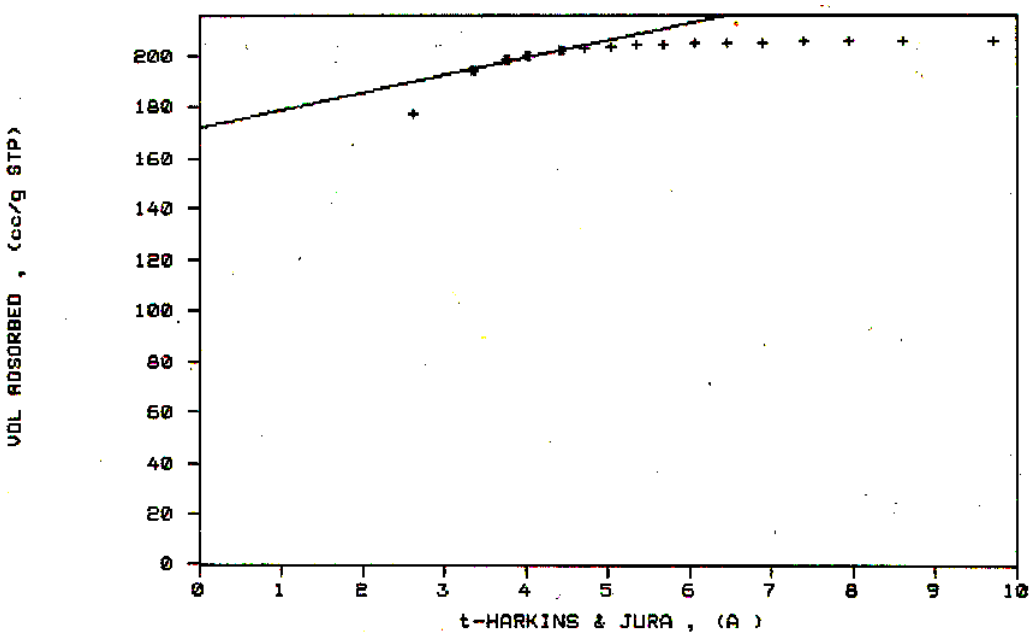

Figure 10: AC1 t-Plot

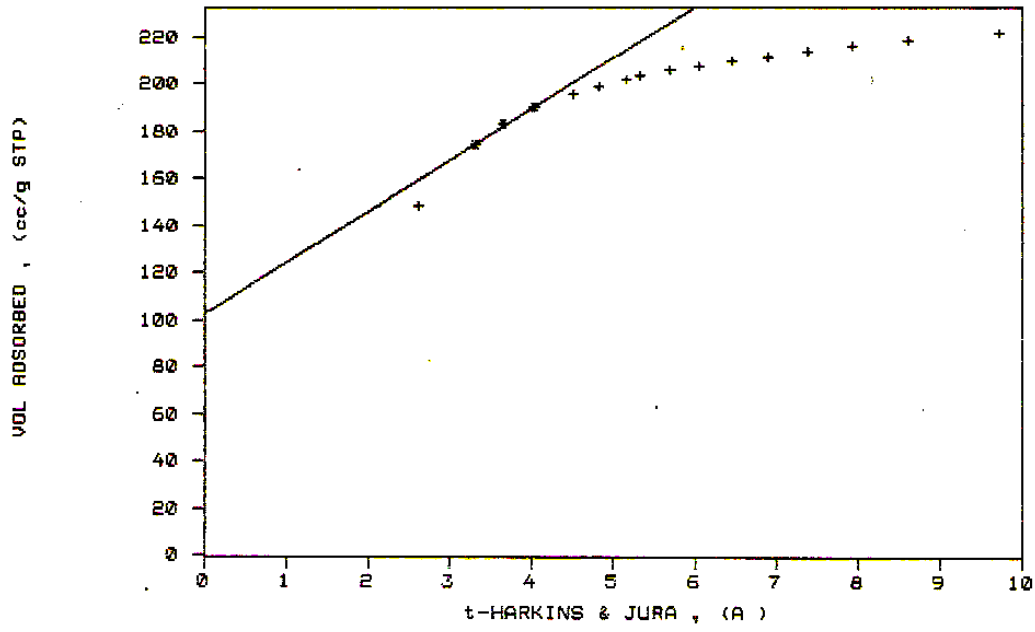

Figure 11: AC2 t-Plot

4.1.2 Morphology Observation Using FESEM

Figure 12, 13 and 14 show the FESEM images of the R&M activated carbon (AC1). As observed from Figure 12 and 13, AC1contains pores in various sizes, ranging from nanometer to micrometer. The ample of pores on the surface is promising and most possible for methane adsorption. The image labeled with arrow in Figure 12 is found as the impurities on the carbon. The impurities can be removed through degasification. As in Figure 13, the activated carbon contains nanopores in the range of 1-100 nm. The pore size should be at least 0.76 nm, which is twice the size of the methane kinetic size, in order for methane gas to travel in and out the pores smoothly. This is important in maximizing the methane delivery. AC1 also contains deep pore, referring to Figure 14. Deep pore would have the possibility to collapse if high pressure is applied.

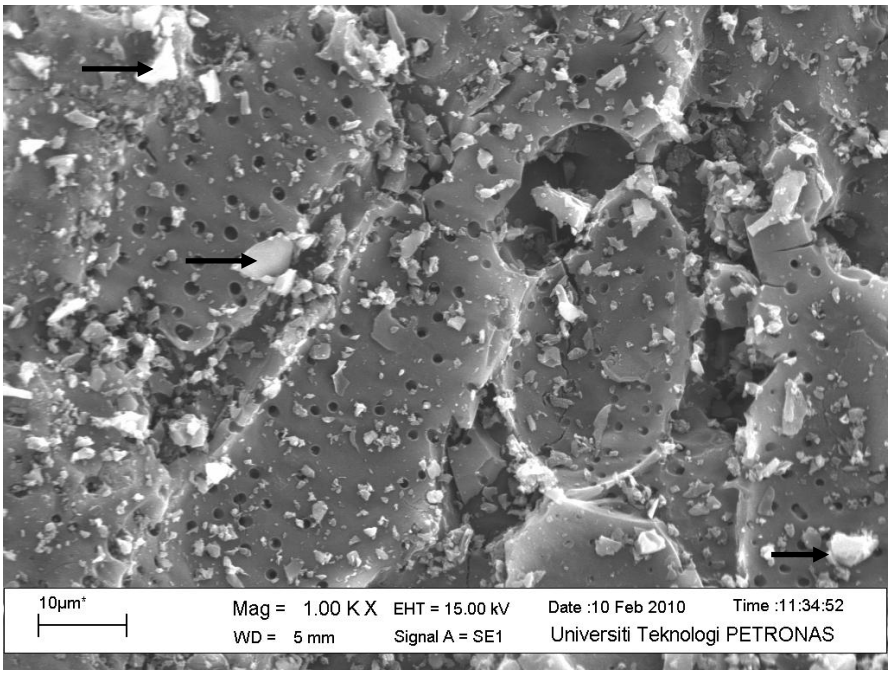

Figure 12: R&M Activated Carbon (AC1)

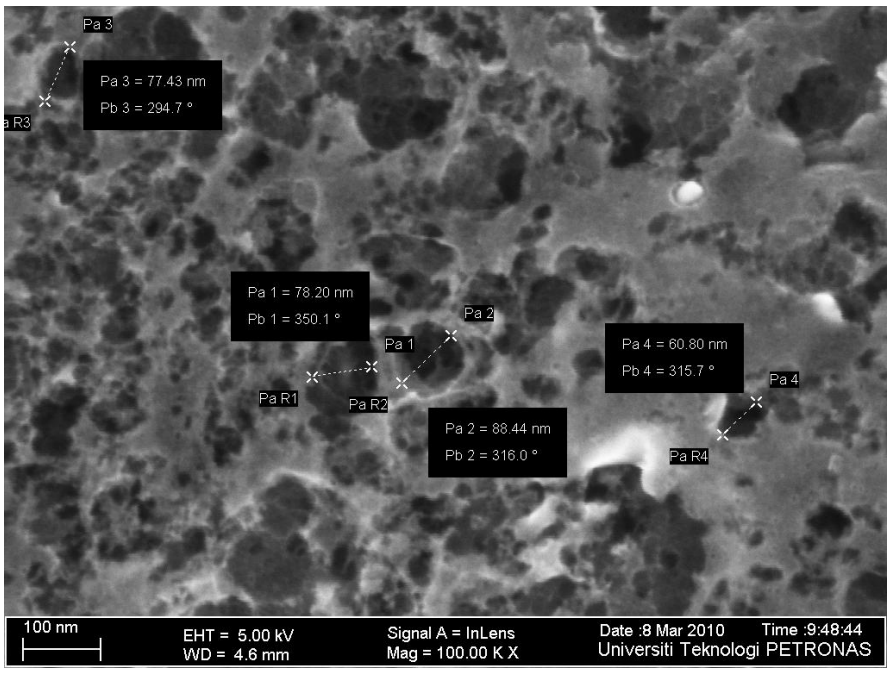

Figure 13: Nanopores on R&M Activated Carbon (AC1)

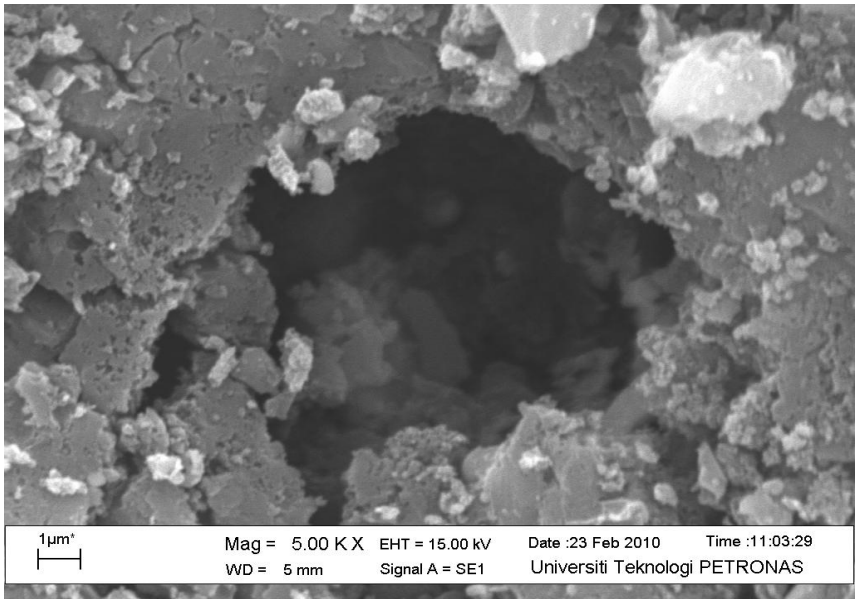

Figure 14: Deep Pore Structure of R&M Activated Carbon (AC1)

Figure 15, 16 and 17 show the FESEM images of Merck Activated Carbon (AC2). Comparing Figure 15 and Figure 12, the pores seem to appear less in AC2 compare to AC1 at the same magnification of 1000X and WD of 5mm. Base on Figure 15 and 16, it is observed that the range of pores on AC2 is in the range of nanometer to micrometer. The pore size should be at least 0.76 nm, which is twice the size of the methane kinetic size, for methane gas to travel in and out the pores smoothly. In figure 17, it shows the image of deep pore existing on AC2. There is a possibility where the deep pores might collapse if high pressure is applied on the AC2.

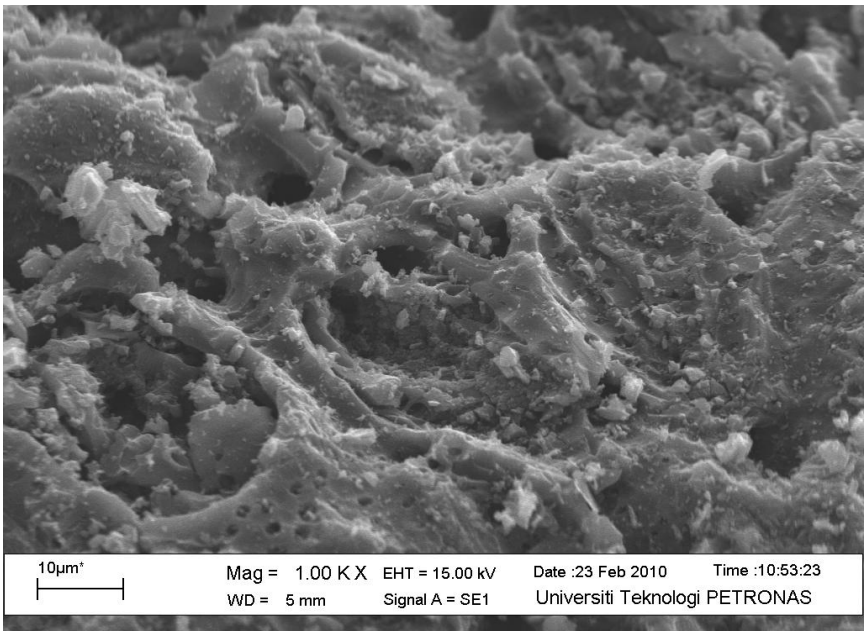

Figure 15: Merck Activated Carbon (AC2)

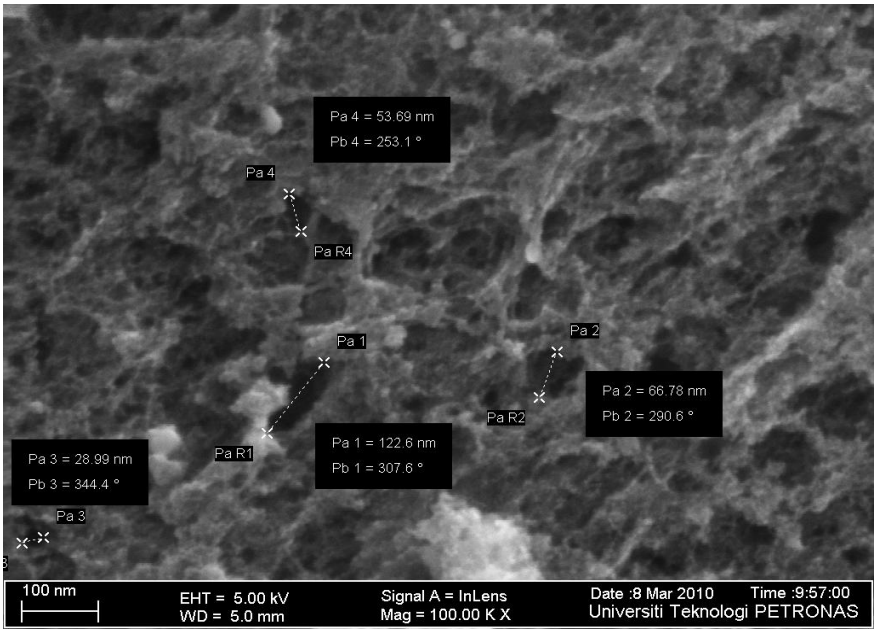

Figure 16: Nanopore on Merck Activated Carbon (AC2)

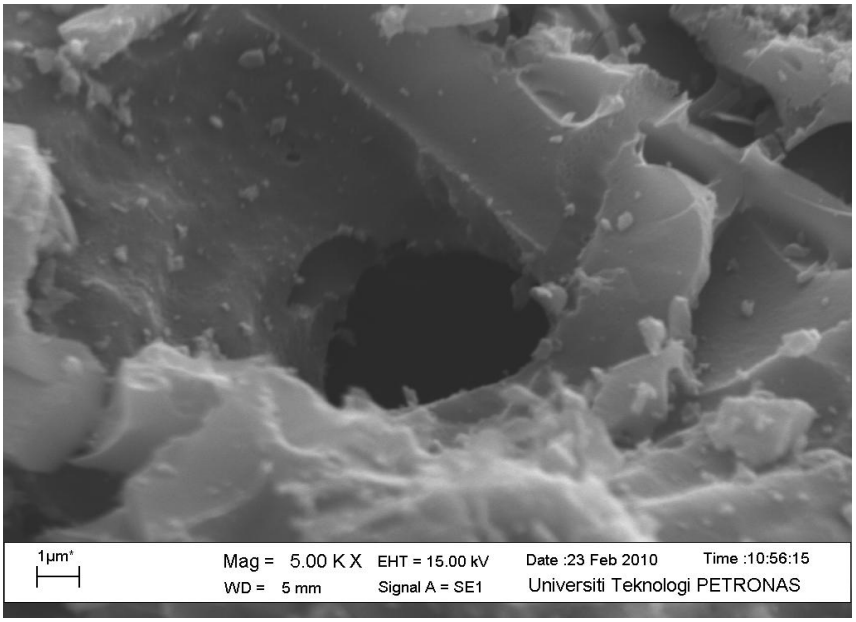

Figure 17: Deep Pore Structure of Merck Activated Carbon (AC2)

4.2 MEASUREMENTS OF GAS ADSORPTION EXPERIMENT

4.2.1 Adsorption Behavior of AC1 During Charging

During the experiments, the column is charged at different pressure and flow rate. From the practical point of view, 20, 40 and 60 bar are chosen as adsorption pressure, and the charge flow rates are 1, 2 and 3 L/min. The amount of AC1 used to fully fill the adsorption column is 235.71 g. The temperature and pressure performance in the column is recorded. The results obtained are time-based result and plotted in the graph. Figure 18, 19 and 20 show the measurement result from the experiment. In the graphs, T1, T2 and T3 correspond to P1, P2 and P3 respectively. The start temperature for every experiment is at ambient temperature, 25°C. Refer Appendix B for the data.

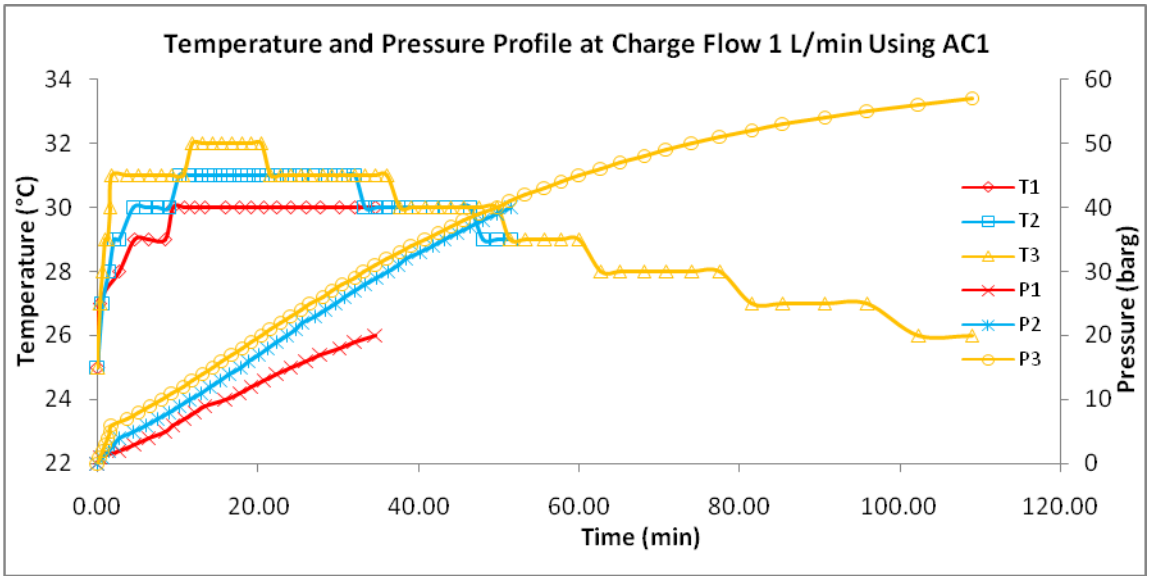

Figure 18: Temperature and Pressure Profile at Charge Flow 1 L/min Using AC1

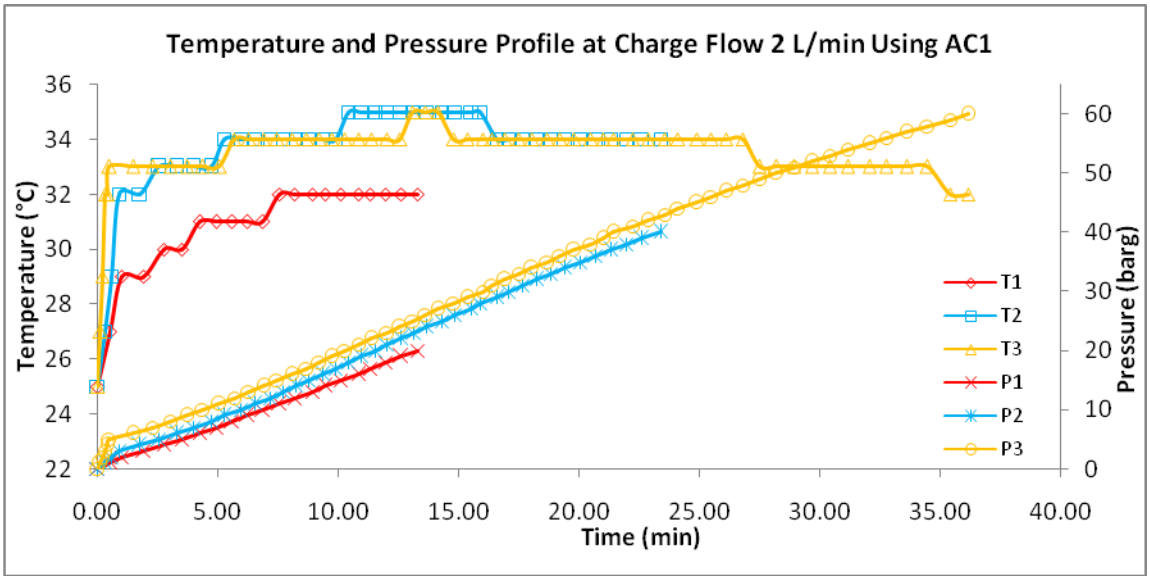

Figure 19: Temperature and Pressure Profile at Charge Flow 2 L/min Using AC1

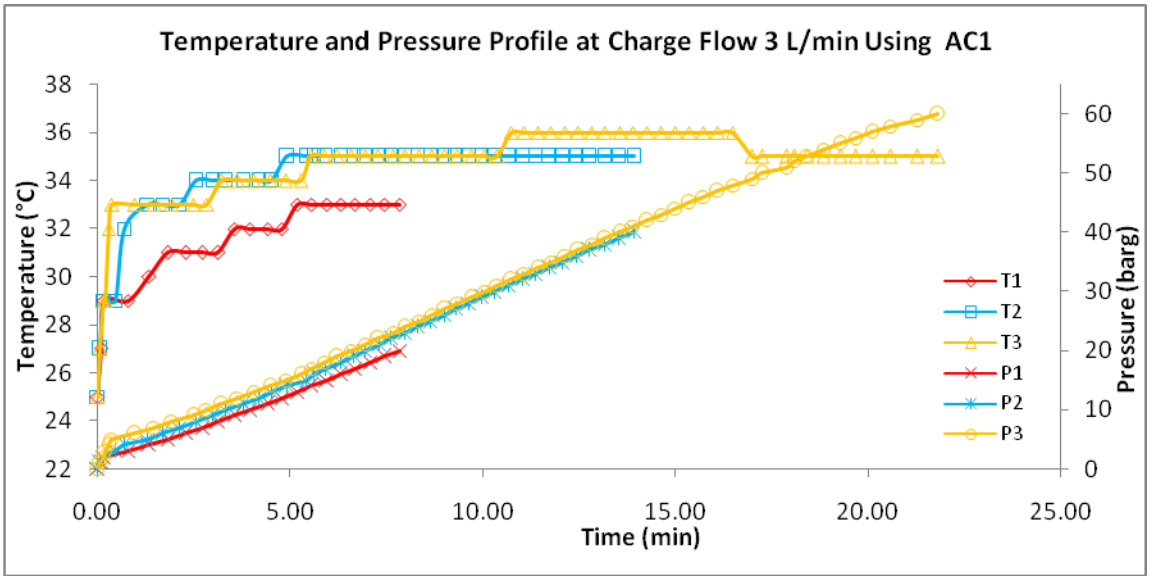

Figure 20: Temperature and Pressure Profile at Charge Flow 3 L/min Using AC1

Comparing the three graphs, Figure 18, 19 and 20 the flow rate methane during the charging will influence the saturation time. Investigate the charge pressure of 60 bar, charge flow of 1 L/min needed 109 minutes to saturate, charge flow rate of 2 L/min needed 36.17 minutes to saturate and 3 L.min charge flow needed only 21.83 minutes to saturate. Higher charge flow rate will decrease the saturation time.

In the adsorption process, it is found that the temperature increases to higher maximum temperature with increases in charge pressure. For example, referring to Figure 20, the charge flow rate at 3 L/min, at 20 bar the temperature can rise to maximum of 33°C, at 40 bar the temperature raised to maximum of 35°C, and at 60 bar the temperature raised to 36°C. This is due to more gas is injected into the column at higher pressure. Therefore, adsorption happens at higher rate and exothermic reaction takes place to release more heat. Moreover, the temperature increases quickly to the maximum at lower charge pressure. At 20bar the temperature increased to 33°C in 5.55 minutes, for 40 bar the temperature increased to 35°C in 4.92 minutes, and for 60 bar the temperature increased to 36°C in 10.38 minutes.

At higher charge flow rate, the maximum temperature the adsorption can reach is higher. Referring to Figure 18, 19 and 20, at charge pressure of 40 bar, charge flow at 1 L/min the temperature raised to maximum 31°C, charge flow at 2 and 3 L/min, the temperature raised to maximum 35°C. At fast fill, the carbon bed temperature rises rapidly because the bed would not have enough time to cool down. Note that at lower charge flow, the temperature during the adsorption tends to rise to the maximum relatively slow and drop again along the adsorption period. This is because the adsorption tends to slow down at higher pressure and less exothermic process occurring. Moreover, the column is not insulated, the heat from the adsorption is dissipated out from the column before it can raise the temperature in the column.

For charge flow at 2 and 3 L/min at charge pressure 20 bar and 40 bar, it seems that the adsorption has not reached the saturation state. This is due to fast charging where the methane gas is not fully adsorbed into the adsorbent even though the column

pressure has reached the same value as the charge pressure. Note that the temperature also increased quickly during the fast charging. Carbon is poor in heat conductivity, therefore the heat is difficult to be dissipated out and remain in the column for some time.

Unlike the slow charging, in Figure 18, the pressure reached to a saturation state and does not vary. This is clearly shown where the curve is deviated from the linear line, even at the end of the curve. At charge flow 1 L/min, for all the different charge pressure (20, 40 and 60 bar), it is considered that the adsorbent has reached the saturation state. Saturation behavior is also shown in charge flow 2 and 3 L/min with charge pressure at 60 bar.

For real application, safety concern is always set as the priority. High pressure and high charge flow would be fast, however the temperature increase is higher and the column would not be fully saturated. On the other hand, low pressure and low charge flow is safer to operate though it would need a long time for charging. Therefore, it is important to charge the column at optimum charge pressure and flow rate.

4.2.2 Adsorption Behavior of AC2 During Charging

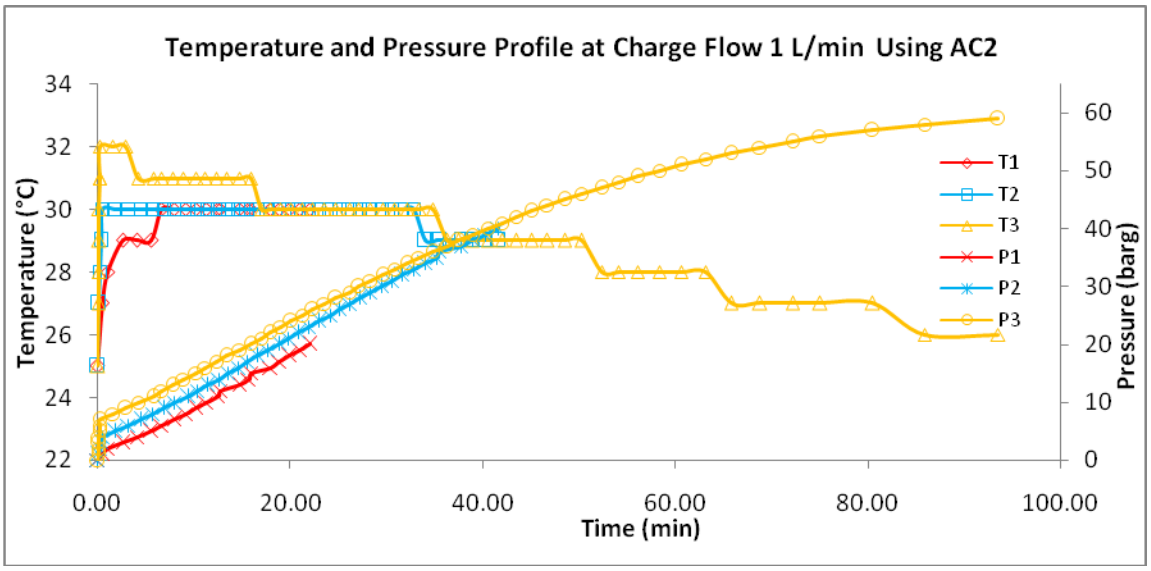

Figure 21: Temperature and Pressure Profile at Charge Flow 1 L/min Using AC2

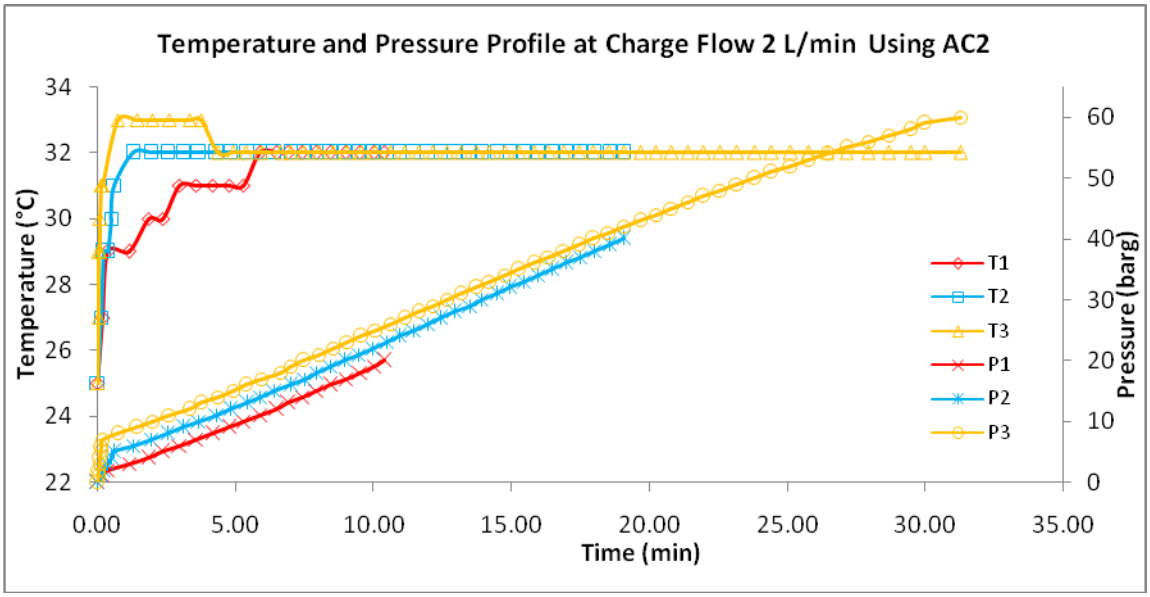

Figure 22: Temperature and Pressure Profile at Charge Flow 2 L/min Using AC2

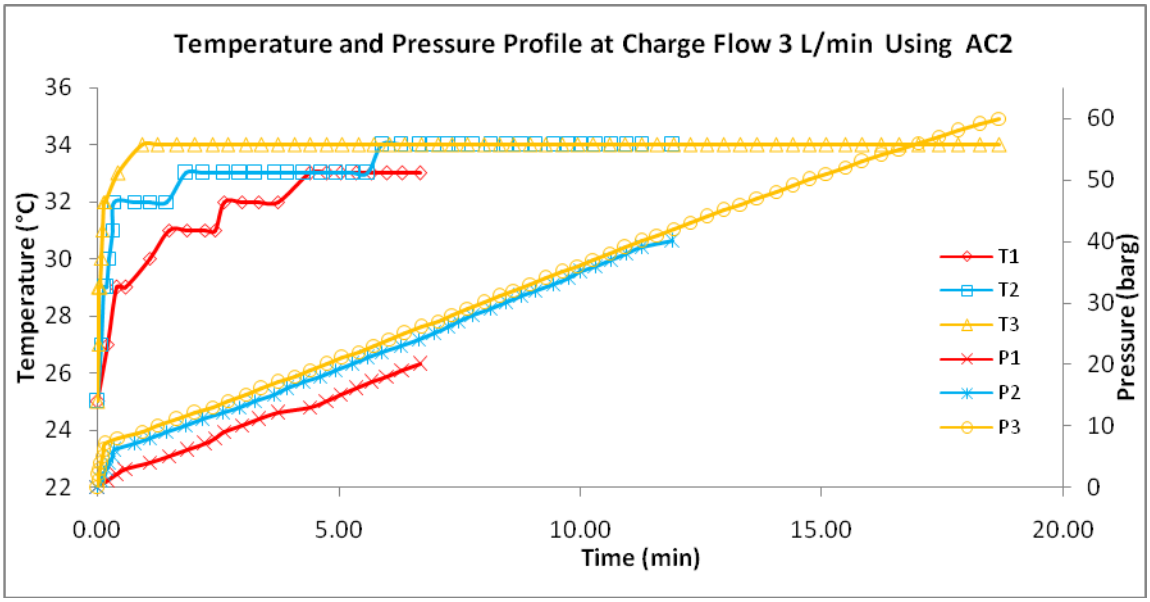

Figure 23: Temperature and Pressure Profile at Charge Flow 3 L/min Using AC2

Comparing the three graphs, Figure 21, 22 and 23 the flow rate methane during the charging will influence the saturation time. Looking at the charge pressure of 60 bar, charge flow of 1 L/min needed 93.58 minutes to saturate, charge flow of 2 L/min needed 31.28 minutes to saturate and 3 L.min charge flow needed only 18.68 minutes to saturate. Higher charge flow rate will decrease the saturation time.

In the adsorption process, it is found that the temperature increases to higher maximum temperature with increases in charge pressure. For example, referring to Figure 23, at charge flow rate of 3 L/min, at 20 bar the temperature can rise to maximum of 33°C, at 40 bar the temperature raised to maximum of 34°C, and at 60 bar the temperature raised to 34°C. This is due to more gas is injected into the column at higher pressure. Therefore, adsorption happens at higher rate and exothermic reaction takes place to release more heat.

At higher charge flow rate, the maximum temperature the adsorption can reach is higher. Using the charge pressure of 40 bar, charge flow at 1 L/min the temperature raised to maximum 30°C, charge flow at 2 L/min the temperature raised to maximum 32°C, at 3 L/min, the temperature raised to maximum 33°C. Note that at lower charge flow, the temperature during the adsorption tends to rise to the maximum and drop again along the adsorption period. This is because the adsorption tends to slow down at higher pressure. The heat from the adsorption is dissipated out from the column before it can raise the temperature in the column.

For charge flow at 1, 2 and 3 L/min at charge pressure 20 bar and 40 bar, it seems the adsorption has not reached the saturation state. This is due to fast charging where the methane gas is not fully adsorbed into the adsorbent even though the column pressure has reached the same value as the charge pressure. Note that the temperature also increased quickly during the fast charging. Carbon is poor in heat conductivity, therefore the heat difficult to dissipate out and remain in the column for some time.

Unlike the slow charging, in Figure 21, at charge pressure 60 bar the pressure reached to a saturation state and does not vary. This is clearly shown where the curve is deviated from the linear line, even at the end of the curve. At charge flow 1 L/min, for charge pressure 60 bar, it is considered that the adsorbent has reached the saturation state. Saturation behavior is also shown in charge flow 2 and 3 L/min with charge pressure at 60 bar.

For real application, safety concern is always set as the priority. High pressure and high charge flow would be fast, however the temperature increase is higher and the column would not be fully saturated. On the other hand, low pressure and low charge flow is safer to operate though it would need a long time for charging. Therefore, it is important to charge the column at optimum charge pressure and flow rate.

4.2.3 Comparison of Adsorption Behavior between AC1 and AC2

Considering charge flow of 1 L/min and 60 bar pressure has better result, comparison on operating behavior is done between AC1 and AC2.

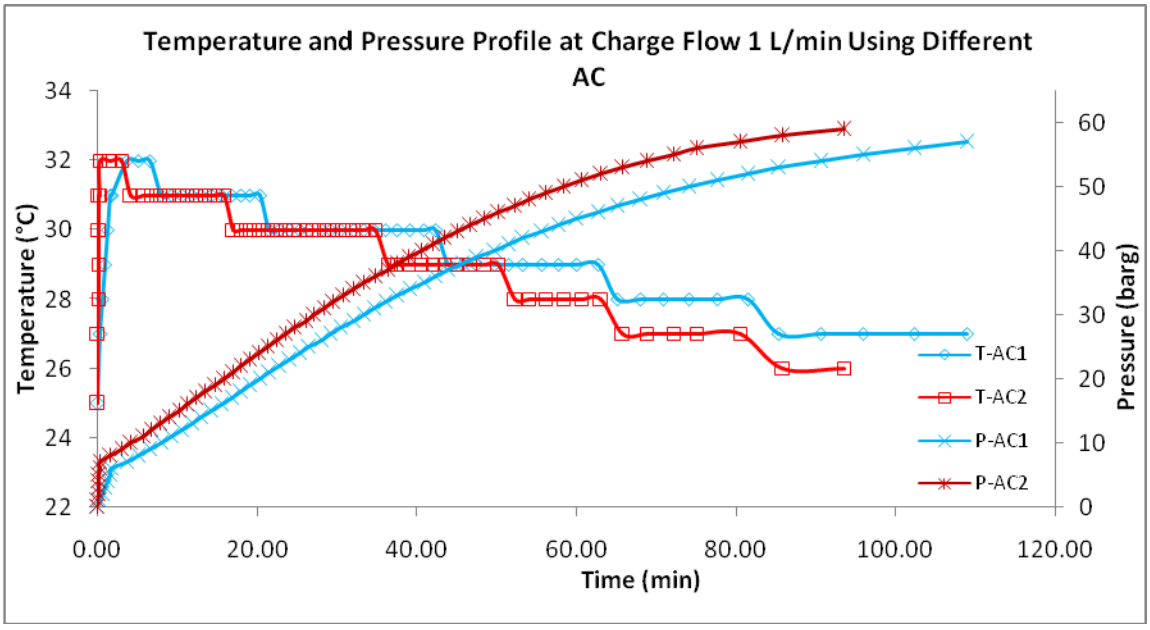

Figure 24: Temperature and Pressure Profile at Charge Flow 1 L/min Using Different AC

Figure 24 shows the behavior profile of temperature and pressure over the adsorption period. The column pressure of AC1 increased slower as compared to the column pressure of AC2. The saturation time of AC1 is 109 minutes while AC2 is 94 minutes. AC1 adsorbs methane slowly and expected to have high capacity for methane adsorption. Total methane injected into AC1 is 109 L while AC2 is 93.58 L. Considering AC1 has larger surface area, micropore volume and micropore area, it is predicted to have higher adsorption capacity.

The temperature drop of AC2 is observed to be more rapid than AC1. The temperature drop is often related to the thermal conductivity of the adsorbent material. Material with high thermal conductivity tends to dissipate heat energy faster. From this point of judgment, AC2 would have higher thermal conductivity than AC1.

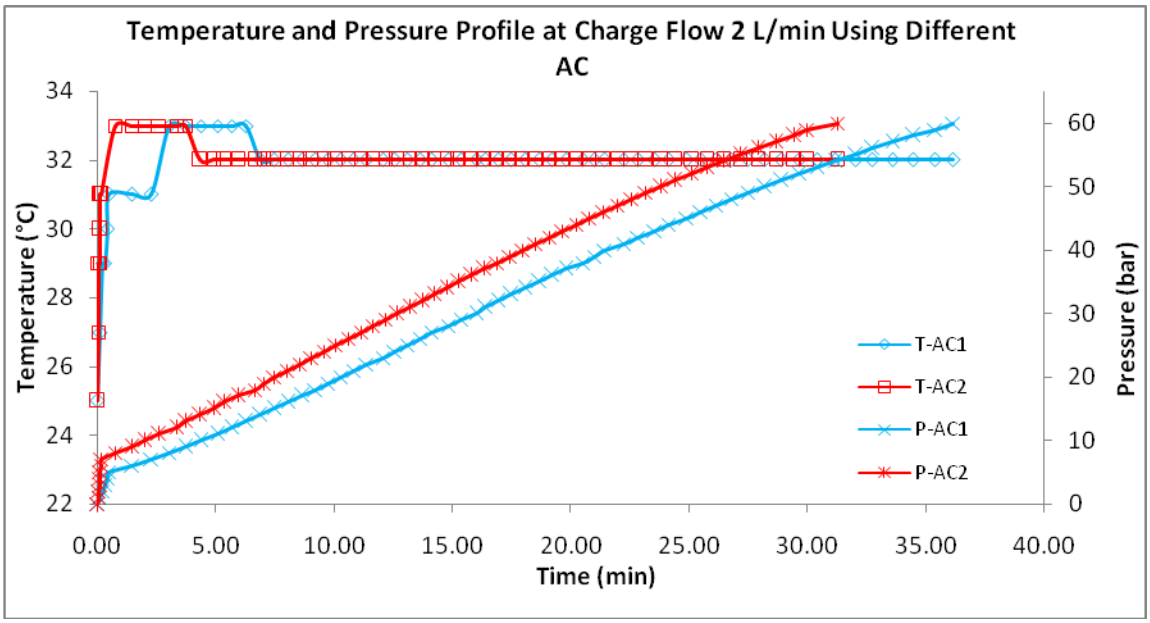

Figure 25: Temperature and Pressure Profile at Charge Flow 2 L/min Using Different AC

Figure 25 shows the temperature and pressure profile of AC1 and AC2 at charge flow rate 2 L/min. From Figure 24 and 25, the temperature of AC2 increases quickly during the adsorption compared to AC1. The rapid rise of temperature is contributed by

the rapid increased of pressure in the column. Comparing Figure 24 and 25, the rapidity increase of pressure in the column is influenced by the charge flow rate.

4.3 ADSORPTION CAPACITY

To determine the amount of methane adsorbed on the adsorbent, it is necessary to measure the dead volume, V_d, which is the free volume (void space). V_d is the difference between V of the container and the volume V_s of the solid adsorbent [12]. In order to calculate Vs, it is important to determine the column volume, mass of adsorbent used to fill the column and real density of adsorbent. Refer Appendix C for the data.

The column volume, V

$$V = \pi r^2 L = \pi(2.25)^2(30) = 477.13\ cm^3 \tag{4.1}$$

The dead volume, V_d [15]

$$V_d = V - \frac{m_s}{\rho_s} \tag{4.2}$$

Assume that the dead volume is always constant throughout the experiment. The number of mol methane in the dead volume is calculated using real gas law at respective adsorption temperature and pressure.

A simple form of virial expansion can determine the compressibility factor, Z [12] as:

$$Z = 1 + \left(\frac{BP_c}{RT_c}\right)\left(\frac{P_r}{T_r}\right) \tag{4.3}$$

In which [12]

$$\left(\frac{BP_c}{RT_c}\right)\left(\frac{P_r}{T_r}\right) = B^0 + 0.0104B^1 \tag{4.4}$$

Where [12]

$$B^0 = 0.083 - \frac{0.422}{T_r^{1.6}} \tag{4.5}$$

$$B^1 = 0.139 - \frac{0.172}{T_r^{4.2}} \tag{4.6}$$

Methane in dead volume, n_d [12]

$$n_d = \frac{PV_d}{zRT} \tag{4.7}$$

Total methane injected into the column, n_T [12]

$$n_T = \frac{Volume\ (L) \times 0.656(kg/m^3)}{16\ kg/kmol} \tag{4.8}$$

Methane adsorbed, $n_{adsorbed}$ [12]

$$n_{adsorbed} = n_T - n_d \tag{4.9}$$

Adsorption capacity [12],

$$Adsorption\ capacity = \frac{n_{adsorbed} \times 16.034\ g/gmol}{mass\ of\ adsorbent\ g} \tag{4.10}$$

Table 5: Activated Carbon Properties

	AC1	AC2
Amount of adsorbent, m_s (g)	204.23	235.71
Adsorbent Real density, ρ_s (g/cm^3)	2.0350	2.1517
Volume of adsorbent, V_s (cm^3)	100.3587	109.5459
Dead Volume, V_d (cm^3)	376.7713	367.5840

T_c of methane is 190.3K and P_c 45.36 is atm.

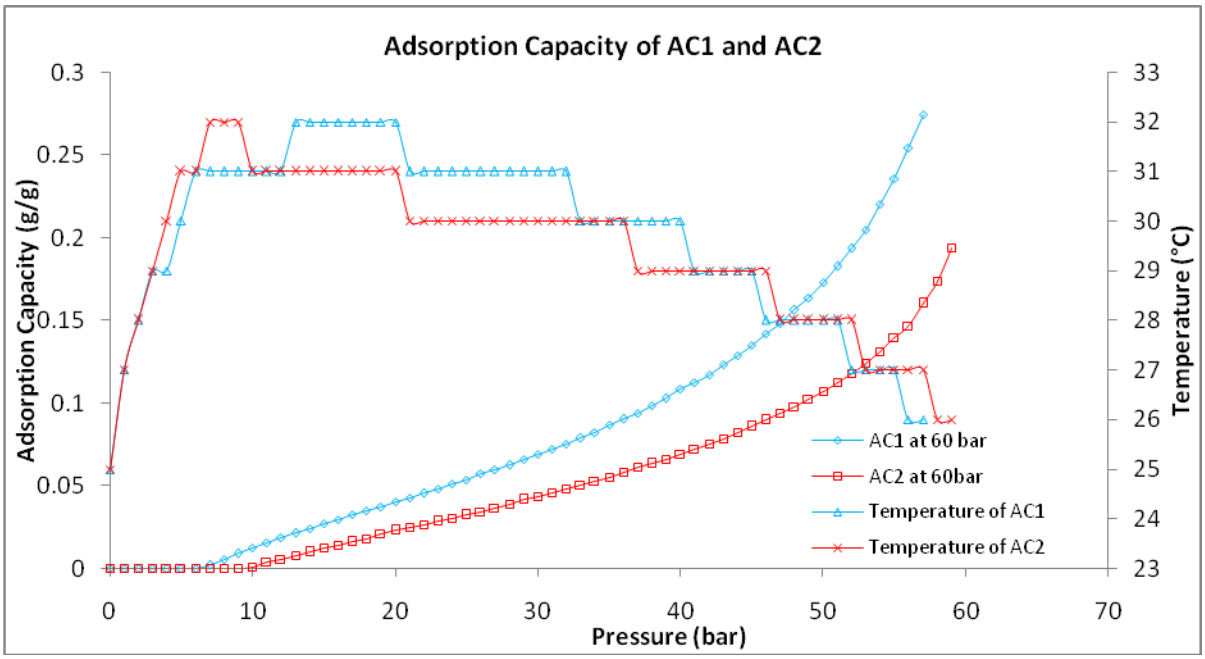

Figure 26: Adsorption Capacity for Different Activated Carbon

Considering charge flow rate 1 L/min and charge pressure 60 bar has the best result, the overall methane adsorption capacity between AC1 and AC2 is compared. Figure 26 shows the adsorption capacity of both the activated carbons at charge pressure 60 bar. As observed, AC1 has higher adsorption capacity than AC2 throughout the adsorption period. This is because AC1 has higher BET surface area, larger micropore area and higher in micropore volume.

Methane adsorption is likely to take place if the average pore size of the adsorbent is larger than 0.76 nm [11]. The kinetic diameter of a methane molecule is 0.38 nm. In order for methane to travel in and out the pore smoothly, the pore size should be at least twice bigger than the kinetic diameter of methane molecule. AC1 and AC2 have average pore size of 1.607 nm and 2.345 nm respectively. Thus, AC1 and AC2 are able to adsorb methane.

From Figure 26, the adsorption capacity tends to increase steeply at the end of the adsorption process for both the activated carbon. This is due to the decrease in temperature at the end of the adsorption. The adsorption capacity is higher at lower temperature [16].

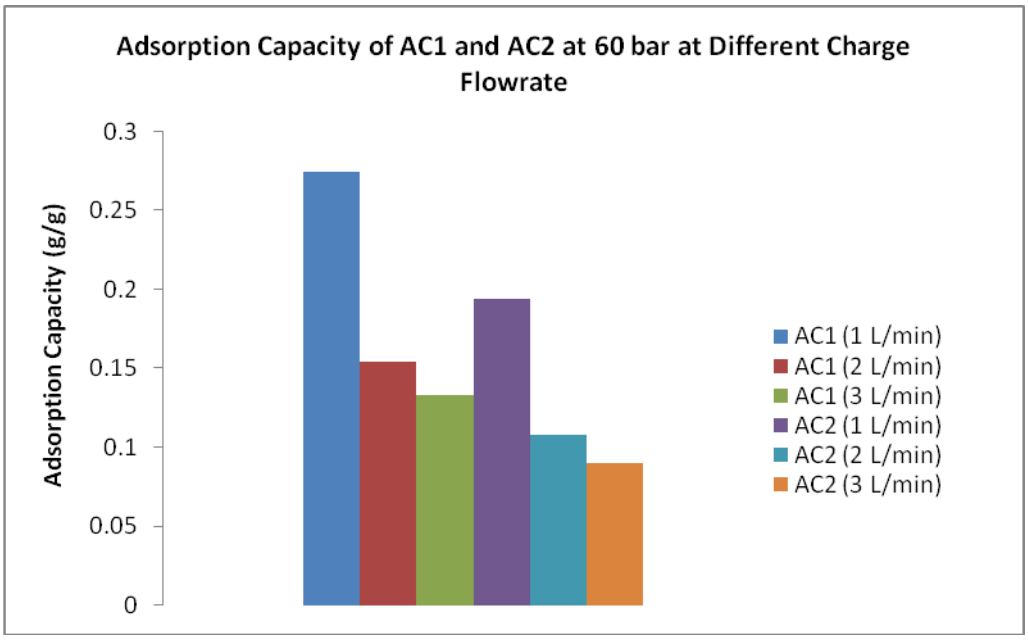

Figure 27: Adsorption Capacity of AC1 and AC2 at 60 bar at Different Charge Flowrate

Figure 27 shows the comparison of methane adsorption capacity of AC1 and AC2 at 60bar and at different charge flow rate. Comparing AC1 alone at different charge flow rate, the adsorption capacity decreases with the increase of charge flow rate. 1 L/min has adsorption capacity at 0.27 g/g, 2 L/min has adsorption capacity at 0.15 g/g

and 3 L/min has adsorption capacity at 0.14 g/g. High charge flow rate cause lower methane uptake because it is a fast charging process and the pressure in the column increases quickly before more methane can settle in the pores. Comparing AC2 alone at different charge flow rate has the same explanation.

AC1 can achieve higher adsorption capacity compared to AC2. At 1 L/min, the adsorption capacity of AC1 is 0.27 g/g and AC2 is 0.18 g/g. At 2 L/min, the adsorption capacity of AC1 is 0.15 g/g and AC2 is 0.11 g/g. At 3 L/min, the adsorption capacity of AC2 is 0.14 g/g and AC2 is 0.09 g/g. Overall, AC1 has higher methane adsorption capacity compared to AC2 at any charge flow rate due to AC1 has relatively larger surface area, micropore area and micropore volume. It is well recognized that better methane adsorption properties will have narrow pore size distribution within the range of 8-15 Å [16]. Larger pore size will provide a weaker potential field for methane adsorption [16]. This is another justification whereby AC2 has lower adsorption capacity due to its average pore size is deviated from the optimum range too much. On the other hand, AC1 has average pore diameter near to optimum pore size range.

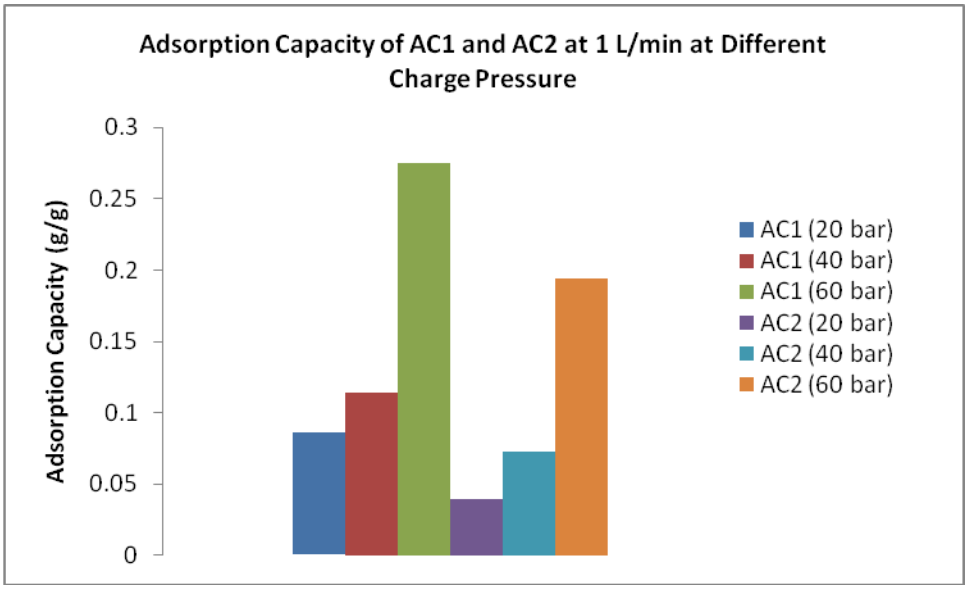

Figure 28: Adsorption Capacity of AC1 and AC2 at 1 L/min at Different Charge Pressure

From Figure 28, comparing AC1 alone at different charge pressure, at 20 bar the adsorption capacity is 0.09 g/g, at 40 bar is 1.1 g/g and at 60 bar is 0.27 g/g. The charge pressure will influence the methane adsorption capacity. At higher charge pressure, more methane is introduced into the column and thus more methane is adsorbed onto the activated carbon. Comparing AC2 alone at different charge pressure has the same explanation.

Comparing between AC1 and AC2, AC1 has higher methane uptake compared to AC2 at the same charge pressure. The difference in methane uptake depends to the surface characteristics between AC1 and AC2. AC1 which has relatively larger surface area, micropore area and micropore volume would have higher adsorption capacity.

4.4 COMPARING ADSORPTION CAPACITY OF DIFFERENT ADSORBENTS

Table 6: Comparison of Methane Adsorption Capacity of AC1 and AC2 with other Adsorbent Materials

Carbon	**Surface Area (m^2/g)**	**Methane Capacity (mg/g)**	**Pressure (barg)**	**Temperature (°C)**
Carbon Lorraine	640	75	34	25
Saran (B)	900	87	34	25
Calgon SGL	900	65	34	25
PX-21, Amoco (Maxsorb)	2671	177	34	25
Electrosynthesis EL	2796	170	34	25
Maxsorb (Grade 30-SPP and Lot 92-05)	3100	211	34	25
AC1	800	84	34	25
AC2	709	54	34	25

Table 6 shows the comparison of methane adsorption capacity between different adsorbent materials. All the materials are carbon. The adsorption capacity Carbon Lorraine, Saran (B), Calgon SGL, PX-21 Amoco (Maxsorb), Electrosynthesis EL and Maxsorb (Grade 30-SPP & Lor 92-05) are adsorbent materials investigated in previous researches.

The adsorption capacity at 34 barg and 25°C for AC1 is 84 mg/g and for AC2 is 54 mg/g. AC1 has higher methane capacity than Carbon Lorraine as AC1 has higher surface area. However, AC1 methane capacity is relatively low compared to other adsorbents due to its small surface area. Although AC2 has higher surface area than Carbon Lorraine, AC2 has large average pore size which is 23.45 Å, which is out of the optimum range of 8 – 15Å for methane adsorption [16]. Base on this result, AC1 and AC2 are not suitable for ANG application due to its low adsorption capacity.

CONCLUSION

AC1 and AC2 are characterized to determine their surface properties. Morphology observation was done to image the surface morphology of these materials. Besides that, other properties such BET surface area, micropore area and micropore volume of the AC1 and AC2 are determined. Both AC1 and AC2 contain nanopores with the average diameter of 1.607 nm and 2.345 nm respectively. The surface properties of the adsorbent will influence the adsorption capacity. High surface area, high micropore volume and optimum pore size will contribute to higher methane adsorption capacity.

In this project, the adsorption behavior during charging of gas has been studied. The temperature profile during adsorption strongly depends on the adsorption pressure and the charge flow rate. Fast charging will result in higher temperature rise compared to slow charging. Adsorbent with high thermal conductivity is preferred for actual application to avoid high temperature rise in the storage. The saturation time also depends on the charge pressure and flow rate. For actual application, safety concern is always set as the priority. High pressure and high charge flow would be fast, however the temperature rise is higher and the column would not be fully saturated. On the other hand, low pressure and low charge flow are safer to operate although it would need a long time for charging. Therefore, selecting suitable charge pressure and flow rate is important to provide optimum and safe operation.

Feasibility of an adsorbent for natural gas storage is based on its practical use, whereby the relation between adsorption pressure relative to its adsorption capacity is measured. From the adsorption capacity comparison, both the AC1 and AC2 have low adsorption capacity compared to other carbon adsorbents at 34 barg and 298K due to low surface area compared to other carbon adsorbents. Thus, selecting the adsorbent with suitable surface characteristics is important for ANG application.

The materials surface properties are characterized to determine its suitability for ANG application and the charging cycle of methane on activated carbon has been studied with different charge pressure and flow rate.

RECOMMENDATIONS

First, the features on SOLTEQ Gas Adsorption Column Unit should be improved. The column K2 should be insulated with heat insulation material. This is to avoid the dissipation of heat during the charging phase. Measurements of temperature rise in the column are important to investigate the feasibility storage of the adsorbent material. The temperature of the adsorption will affect the adsorption capacity. With this improvement, the equipment can be used for adsorption isotherm experiment.

Second, UTP should build gas storage equipment for volumetric measurement. Since the unit for my experiment now is a gas adsorption unit specifically for separation process, it is rather complicated to be used as gas storage unit. Therefore, to build a unit of gas storage equipment would benefit the future research in related areas.

REFERENCES

[1] J. ALCA~Z-MONGE, M. A. DE LA CASA-LILLO, D. CAZORLA-AMOR& and A. LINARES-SOLANO., 1997, "Methane Storage In Activated Carbon Fibres," *Carbon* **35(2):** 291-297

[2] L.L. Vasiliev, L.E. Kanonchik, D.A. Mishkinis., M.I. Rabetsky, 2000, "Adsorbed Natural Gas Storage and Transportation Vessels," *Int. J. Therm. Sci.* **39(2000):** 1047-1055

[3] S. Biloe[a], V. Goetz[a,*], S. Mauran[b]., 2000, "Characterization of adsorbent composite for methane storage," *Carbon* **39(2001):** 1653-1662

[4] S. Biloe´[a], V. Goetz[a,]*, A. Guillot[b]., 2001, "Optimal design of an activated carbon for an adsorbed natural gas storage system," *Carbon* **40(2002):** 1295-1308

[5] M. Bastos-Neto a, D.V. Canabrava a, A.E.B. Torres a, E. Rodriguez-Castello´n b, A. Jime´nez-Lo´pez b, D.C.S. Azevedo a,*, C.L. Cavalcante Jr.a., 2006, "Effects of textural and surface characteristics of microporous activated carbons on the methane adsorption capacity at high pressures," *Applied Surface Science* **253 (2007):** 5721-5725

[6] S. Biloe´[a], V. Goetz[a,]*, A. Guillot[b]., 2001, "Optimal design of an activated carbon for an adsorbed natural gas storage system," *Carbon* **40(2002):** 1295-1308

[7] Danna, A.B.M, Iyuke, S.E**., Fakhrul_razi, A., Chuah T.G., Atieh, M.A., and Al-Khatib. M.F., 2003, "Synthesis and Characterization of Carbon Nano-Structures for Methane Storage," *Environmental Informatics Archieves* **1(2003):** 597-605

[8] Rouquerol, F., Rouquerol, J., and Sing, K. 1999. *Adsorption by Powder Porous Solids*, New York, Academic Press

[9] G. Q. Lu and X. S. Zhao. 2004. *Nanoporous Materials Science and Engineering,* **(4),** New York, Imperial College Press

[10] Rolando M.A. Roque-Malherbe, 2007, *Adsorption and Diffusion in Nanoporous Materials*, New York, CRC Press

[11] V.C. MENON, S. KOMARNENI, 1997, "Porous Adsorbents for Vehicular Natural Gas Storage: A Review," *Journal of Porous Material* **5(1998):** 43-58

[12] E. Salehi, V. Taghikhani*, C. Ghotbi, E. Nemati Lay, A. Shojaei, 2007, "Theoretical and Experimental Study on the Adsorption and Desorption of Methane by Granular Activated Carbon at 25°C," *Journal of Natural Gas Chemistry* **16(2007):** 415-422

[13] Alejandro Saez*, Mario Toledo, 2008, "Thermal effect of the adsorption heat on an adsorbed natural gas storage and transportation systems," *Applied Thermal Engineering* **29(2009):** 2617-2623

[14] Professor Marc Donohue. 7 Sept 2009 http://www.nigelworks.com/mdd/PDFs/NewClass.pdf

[15] Zainal Zakaria. 2006, *The Development of Adsorbent Based Natural Gas Storage For Vehicle Application*, Ph.D. Thesis, Universiti Teknologi Malaysia, Malaysia

[16] Isabel A.A.C. Esteves, Marta S.S. Lopes, Pedro M.C. Nunes, Jose P.B. Mota*, 2008, "Adsorption of Natural Gas and Biogas Components on Activated Carbon," Separation and Purification Technology **62(2008)**: 281-296

APPENDIX

APPENDIX A

APPENDIX B

APPENDIX C